Chinese Chemical Letters 37 (2026) 111120

Contents lists available at ScienceDirect

Chinese Chemical Letters

journal homepage: www.elsevier.com/locate/cclet

Remediation of characteristic contaminants in groundwater of chemical industrial by the activation of PMS: Recent developments and challenges-a mini-review

Yingnan Duan[a], Jinyu Liu[b], Qian Liu[a], Tianhao Li[a], Hexiang Zhao[a,*], Zhurui Shen[a,*]

[a] School of Materials Science and Engineering and Smart Sensing Interdisciplinary Science Center, Nankai University, Tianjin 300350, China
[b] Baotou Animal Husbandry and Aquatic Products Promotion Service Center, Inner Mongolia 014010, China

ARTICLE INFO

Article history:
Received 21 January 2025
Revised 11 March 2025
Accepted 19 March 2025
Available online 20 March 2025

Keywords:
Advanced oxidation processes (AOPs)
In-situ chemical oxidation
PMS
Groundwater contamination
Characteristic pollutants

ABSTRACT

Groundwater is a key part of the terrestrial ecosystem, but it is vulnerable to pollution in the context of chemical industry development. Treating contaminated groundwater is challenging due to its stable water quality, hidden contamination, and complex treatment requirements. Current research focuses on advanced treatment technologies, among which the advanced oxidation process (AOPs) of peroxomonosulfate (PMS) has great potential. Although there are many reviews of PMS-based AOP, most of them focus on surface water. This review aims to explore the activation reaction of PMS to groundwater by *in-situ* chemical oxidation (ISCO) technology, further study the reaction mechanism, compare the treatment effect of characteristic pollutants in the groundwater of the chemical industry park, propose new activation methods and catalyst selection, and provide guidance for future groundwater treatment research.

© 2025 Published by Elsevier B.V. on behalf of Chinese Chemical Society and Institute of Materia Medica, Chinese Academy of Medical Sciences.

1. Introduction

Groundwater is important component of the terrestrial ecosystem, which plays a very critical role in the natural environment and human life [1–3] . However, with the rapid development of the chemical industry, the relatively backward environmental protection technology and awareness, the imperfect policies, regulations and supervision, and the urban expansion changing the pattern of land and water resources, the groundwater in the chemical park are vulnerable to various pollutants, such as heavy metal ions (HMIs), total petroleum hydrocarbon (TPHs), benzene derivatives (BTEX), chloroalkane ((Ar)R-Cl) [4]. This makes effective removal of contaminants from groundwater poses a significant challenge. Different from the treatment of surface water, surface water is in full contact with the outside world, the water quality changes frequently, and is susceptible to a variety of pollution sources, but the dissolved oxygen and microbial activity are high, which is conducive to treatment [5,6]. The treatment technology is mature, the construction and operation of facilities are relatively easy and the cost is low [1,7]. The groundwater quality is relatively stable, but the hidden pollution is difficult to detect in time, the microbial activity is low, and the re-injection or discharge after treatment is limited. So the treatment technology of groundwater is complex. ICSO is a relatively common method. However, it needs to overcome problems such as complex geological conditions. It is difficult to determine the source of pollution and the diffusion path, and the repair cycle is long. These factors result in difficult treatment and high costs [8]. Therefore, it is of great significance to develop efficient treatment measures of groundwater treatment. The properties between groundwater and surface water are listed in Table 1.

Current research mainly focuses on advanced treatment technologies capable of reducing the hazard levels of contaminated groundwater to acceptable standards. Various methods, including adsorption [9,10], coagulation [11], chemical precipitation [12,13], and electrodialysis [14], are extensively studied. Among these techniques, advanced oxidation processes (AOPs) stand out for their ability to generate reactive species, such as free radicals and non-radicals including hydroxyl radical ($^{\bullet}OH$), superoxide radical ($^{\bullet}O_2^-$), singlet oxygen ($^1O_2$), and sulfate radical ($^{\bullet}SO_4^-$). These highly reactive radicals/non-radicals are capable of breaking the covalent bonds of persistent organic pollutants, thereby mineralizing or degrading the target contaminants. This mechanism is applicable to virtually all organic pollutants, highlighting the versatility and effectiveness of AOPs in contaminant removal. H_2O_2, peroxyacetic acid (PAA) and Persulfate (PS) are usually used as oxidizing agents. The PS includes peroxydisulfate (PDS, $S_2O_8^{2-}$) and peroxomonosulfate (PMS, SO_5^{2-}) is a commonly used oxidant, due to high stability,

* Corresponding authors.
E-mail addresses: zhx980417@163.com (H. Zhao), shenzhurui@nankai.edu.cn (Z. Shen).

https://doi.org/10.1016/j.cclet.2025.111120
1001-8417/© 2025 Published by Elsevier B.V. on behalf of Chinese Chemical Society and Institute of Materia Medica, Chinese Academy of Medical Sciences.

Table 1
The comparison of the properties between groundwater and surface water.

Characteristic	Groundwater	Surface water
Temperature	Relatively stable, with little change	Affected by the external climate and fluctuates greatly
Hardness	It could be higher, depending on the minerals in the underground rock	It changes greatly and is affected by the surrounding environment and human activities
Mobility	Relatively weak, slow replenishment	Strong liquidity, easy to flow and spread
Self-cleaning capacity	Weak, more affected by the environment	Strong, conducive to the self-purification of water and material transport

Table 2
Oxidation potential of some common oxidants.

Oxidant	Standard reduction potential (E^0) (V_{NHE})
Fluorine (F_2)	3.0
Hydroxyl radical ($^{\bullet}OH$)	2.8
Sulfate radical ($^{\bullet}SO_4^-$)	2.5–3.1
Ozone (O_3)	2.1
Persulfate ($S_2O_8^{2-}$)	2.1
Peroxymonosulfate (HSO_5^-)	1.82
Hydrogen peroxide (H_2O_2)	1.8
Permanganate (MnO_4^-)	1.68
Chlorine dioxide (ClO_2)	1.5
Chlorine (Cl_2)	1.4

in-expensive and high water solubility [15]. PDS has a symmetric structure with a symmetrical charge distribution, whereas the peroxide bond in PMS is asymmetric, and the peroxide bond attached to the hydrogen is positively charged. Therefore, non-polar PMS is more susceptible to attack by nucleophilic substances in groundwater. The presence of background groundwater constituents, such as Cl^- and HCO_3^-, makes the oxidation efficiency of PMS superior to that of PDS in some cases [16]. The reaction of PMS with natural nucleophiles promotes the decomposition of PMS, enhancing the yields of $^{\bullet}SO_4^-$, $^{\bullet}OH$, and $^1O_2$. So, PMS has emerged as a potential oxidant for the remediation of groundwater.

There are many comprehensive reviews on PMS-based AOPs at the current stage, covering a wide range of detailed perspectives [17–19]. However, most of these reviews tend to focus primarily on two representative aspects: The selection of catalysts and methods of activation for surfacewater. This comparison thoroughly explored the pathways of both free radical and non-radical generation during the reactions. Regarding the selection of catalysts, the scope is much broader, encompassing a wide variety of materials, such as carbon-based materials [20,21], MOFs [22,23], LDHs [24], metal-based or non-metal-based catalysts [25–30], aerogel [31]. Given the difference in nature with surface water, it will be important to focus on the following seven aspects: degradation kinetics, water matrices, selectivity, temperature, pH, by-products, and electrical demand for groundwater management.

Herein, this timely mini-review aims to meticulously explore the activation reactions of PMS for groundwater. Firstly we introduce the PMS reaction mechanisms deeply, including modes of free radical production under different activation modes. Then, a comparison of the effects of PMS-based AOPs on characteristic pollutants in the groundwater of chemical industrial parks (such as aromatic compounds, chlorinated hydrocarbons, petroleum hydrocarbons, persistent organic pollutants, heavy metals), revisiting the most recent and representative achievements and progress over the past five years. It presents the performance of PMS-based AOPs in treating different pollutants, highlighting emerging activation methods for PMS and the selection of new catalysts. This provides insights into the efficient, selective advanced oxidation treatment of characteristic pollutants in the groundwater of chemical industrial parks, offering significant guidance for future research.

2. Mechanisms of PMS-based AOPs reactions

Activating PMS is a crucial step that enables its reactivity in the treatment of characteristic pollutants. Typically, PMS can be activated through various methods, including metal ions activation, thermal activation, irradiation activation, and alkaline activation. The redox potential of sulfate radical produced through the activation of PMS depended on the activation methods [32]. Oxidation potential of some common oxidants are listed in Table 2. In this part, we summarize the activation processes of PMS and compares how different activation methods influence the pathways of reactive oxygen species generation. Finally, we propose the potential of PMS for groundwater management.

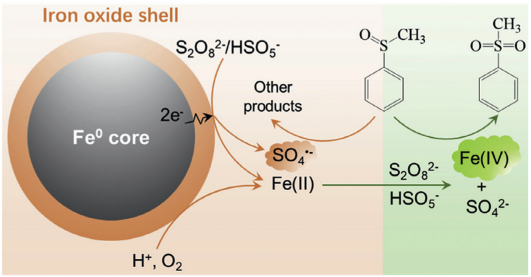


Fig. 1. Pathways of active species generation and final action on pollutants in the ZVI/PMS system. Reprinted with permission [38]. Copyright 2020, Elsevier.

2.1. Mechanisms of transition metal activation

In both supported and unsupported metal-based catalysts, metal species are acknowledged as the catalytic centers. Metal species, due to their diverse geometric structures, display distinct catalytic performances during heterogeneous catalytic reactions. The geometric configuration of metal species (such as nanoparticles, nanoclusters and single atoms) can significantly influence factors such as reactant adsorption, activation, and product desorption [33–35]. In the process of transition metal activation of PS/PMS reactions, metal ions (M^{n+}) can be dispersed freely in the solution, reacting with PS/PMS to produce a large amount of $^{\bullet}SO_4^-$, as illustrated in the following reactions (Eqs. 1 and 2).

$$HSO_5^- + M^n \rightarrow M^{n+1} + {}^{\bullet}SO_4^- + OH^- \quad (1)$$

$$S_2O_8^{2-} + M^{n+} \rightarrow M^{n+1} + {}^{\bullet}SO_4^- + SO_4^{2-} \quad (2)$$

Iron-based catalysts, as a focal point of research, serve as an example to detail the generation of reactive species under the activation of PMS by Fe^0 and Fe^{2+}. The zero-valent iron/PMS (ZVI/PMS) system exhibits strong reductive capabilities [36,37], and the reaction process is complex [38]. As shown in Fig. 1, Fe^0 initially transforms into Fe^{2+} under acidic conditions, which then participates in the reaction to generate SO_4^{2-} and $^{\bullet}SO_4^-$. A portion of Fe^0 also directly reacts with PMS, producing $^{\bullet}SO_4^-$ and OH^-. The reaction equations are shown in Eqs. 3-6.

$$Fe^0 + 2H^+ \rightarrow Fe^{2+} + H_2 \quad (3)$$

$$Fe^0 + HSO_5^- \rightarrow Fe^{2+} + OH^- + SO_4^{2-} \quad (4)$$

$$Fe^0 + 2HSO_5^- \rightarrow Fe^{2+} + 2{}^{\bullet}SO_4^- + 2OH^- \quad (5)$$

$$Fe^{2+} + HSO_5^- \rightarrow Fe^{3+} + SO_4^{2-} + {}^{\bullet}SO_4^- \quad (6)$$

2.2. Mechanisms of thermal activation

Thermal activation represents another effective pathway for PMS activation, involving various forms such as heating or ultrasound. By absorbing heat, when the energy surpasses the bond energy of the O–O bond in PMS, which is between 140 kJ/mol and 213.3 kJ/mol, PMS can be successfully activated (>50 °C). The O–O bond in PMS breaks, forming $^{\bullet}SO_4^-$. Additionally, the thermal activation process generates a significant amount of $^{\bullet}OH$ radicals because $^{\bullet}SO_4^-$ can convert into $^{\bullet}OH$ during the heating process, as indicated in the recation (Eqs. 7 and 8) [39–41].

$$HSO_5^- \rightarrow {}^{\bullet}SO_4^- + {}^{\bullet}OH \quad (7)$$

$$SO_4^- + H_2O \rightarrow SO_4^{2-} + {}^{\bullet}OH + H^+ \quad (8)$$

2.3. Mechanisms of irradiation activation

Ultraviolet (UV) irradiation is considered an economical and efficient method within radiation activation techniques for degrading organic pollutants in wastewater [42–44]. The most commonly used wavelength is 254 nm. Some reviews suggest that while the activation of H_2O_2 and O_3 by UV primarily generates $^{\bullet}OH$ radicals, activating PMS predominantly produces $^{\bullet}SO_4^-$. For the degradation of organic pollutants, $^{\bullet}SO_4^-$ demonstrates superior efficacy. The recognized activation mechanisms are broadly categorized into two types: one involves the input of UV energy causing O–O bond breakage, and the other involves water molecules absorbing the energy produced by UV irradiation, which then transfer electrons and activate PMS through electron conduction. The reaction equations for these two mechanisms are as in Eqs. 9-11. Furthermore, the effectiveness and non-polluting nature of UV irradiation activation make it notably representative. Beyond UV irradiation, methods such as gamma radiation (within the UV absorbance range) and ultrasound have also been proven capable of activating PMS [45].

$$HSO_5^- \rightarrow {}^{\bullet}SO_4^- + {}^{\bullet}OH \quad (9)$$

$$H_2O \rightarrow {}^{\bullet}H + {}^{\bullet}OH \quad (10)$$

$$HSO_5^- + {}^{\bullet}H \rightarrow {}^{\bullet}SO_4^- + H_2O \quad (11)$$

2.4. Mechanisms of alkaline activation

The pH value plays a crucial role in the activation steps of PMS activation, primarily affecting the equilibrium between $^{\bullet}O_2^-$ and $^{\bullet}HO_2$. Typically, under acidic conditions, $^{\bullet}O_2^-$ tend to react with H^+ in the solution to form $^{\bullet}HO_2$. Conversely, under alkaline conditions, $^{\bullet}HO_2$ is inclined to decompose, producing $^{\bullet}O_2^-$. Furthermore, under alkaline conditions, $^{\bullet}SO_4^-$ can also generate $^{\bullet}OH$ through further reactions. The alkaline activation mechanisms of PDS and PMS are similar. Here, only the activation mechanism equations for PMS are displayed (Eqs. 12-23). From these equations, the generation of $^1O_2$ can be observed, which is also an efficient reactive species in the degradation of organic pollutants [40,46].

$$HSO_5^- + H_2O \rightarrow H_2O_2 + HSO_4^- \quad (12)$$

$$HSO_5^- \rightarrow H^+ + SO_5^{2-} \quad (13)$$

$$SO_5^{2-} + H_2O \rightarrow H_2O_2 + SO_4^{2-} \quad (14)$$

$$H_2O_2 \rightarrow H^+ + O_2H^- \quad (15)$$

$$H_2O_2 + OH^- \rightarrow H_2O + O_2H^- \quad (16)$$

$$HSO_5^- + O_2H^- \rightarrow H_2O + {}^{\bullet}SO_4^- + {}^1O_2 \quad (17)$$

$$H_2O_2 \rightarrow 2{}^{\bullet}OH \quad (18)$$

$$^{\bullet}OH + H_2O_2 \rightarrow {}^{\bullet}HO_2 + H_2O \quad (19)$$

$$^{\bullet}HO_2 \rightarrow H^+ + {}^{\bullet}O_2^- \quad (20)$$

$$^{\bullet}OH + {}^{\bullet}O_2^- \rightarrow {}^1O_2 + OH^- \quad (21)$$

$$2{}^{\bullet}O_2^- + 2H^+ \rightarrow {}^1O_2 + H_2O_2 \quad (22)$$

$$HSO_5^- + SO_5^{2-} \rightarrow HSO_4^- + {}^{\bullet}SO_4^- + {}^1O_2 \quad (23)$$

2.5. Mechanisms of coupling activation

At the current stage of research, a more common approach is to combine various activation methods. Given the individual advantages and disadvantages of metal, radiation, thermal, and alkaline activation methods, the combination of these approaches is increasingly attracting researchers' attention. With industrial development in mind, Swapnil K. *et al.* designed several reactors that synergize ultrasound (US) with thermal, ultraviolet, and other PMS activating substances [47]. He discussed the potential applications of these devices in water treatment, sterilization and disinfection, wastewater disposal, soil contamination, and sludge treatment. Experimental results showed that the combined activation with US significantly improved degradation rates. Additionally, the use of fewer chemicals and shorter treatment times also led to lower operational costs. Swapnil K. attributed the excellent performance to the synergistic effects of radical reactions and thermal action. Furthermore, the unique design of the reactor, which generates intense turbulence, optimizes oxidative contact and mass transfer rates. Du *et al.* applied vacuum ultraviolet (VUV) combined with O_3 for the activation of PMS in the degradation system of Levofloxacin (LEV) [48]. The research results indicated that compared to single activation, the coupled activation increased the degradation rate by 1.67–18.79 times while reducing energy consumption by 22.6 %–88.1 %. $^{\bullet}OH$ and $^{\bullet}SO_4^-$ radicals served as the main reactive oxygen species. This provides a solid guideline for the coupled activation process of PMS.

The activation of PMS is not limited to the aforementioned methods [49–51], and the impact of different activation approaches on degradation performance can vary greatly. Considering the complexity of groundwater environment in chemical industry park, higher requirements are put forward for treatment methods. Therefore, *in-situ* treatment can be used through PMS activation technology. PMS eliminates the need to pump groundwater to the surface, cutting costs related to equipment and pipelines while minimizing environmental disturbance. The reactive media within PMS can efficiently remove various pollutants like heavy metals and organic compounds, and its continuous purification ability ensures long-term effectiveness. Operationally, PMS is simple, requiring little oversight, and has low maintenance costs. Environmentally, PMS can reduce secondary pollution risks and promoting ecological restoration. Moreover, it can be customized to fit different geological and pollution conditions, and has a broad application scope for different types of groundwater pollution.

3. Remediation of characteristic contaminants in groundwater by PMS

Over the past five years, various technologies have been employed to activate PMS for treating contaminated groundwater,

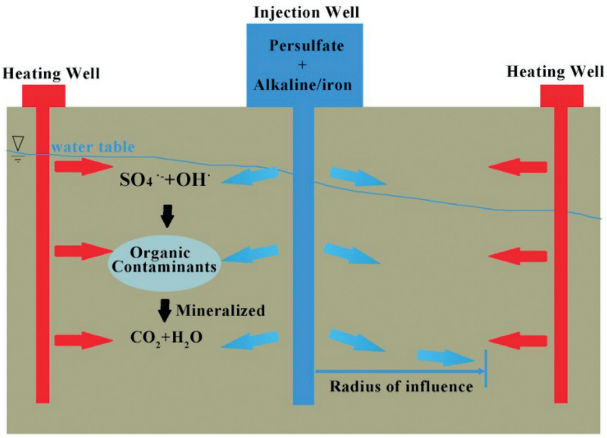


Fig. 2. The application mechanism of ISCO using persulfate. Reprinted with permission [52]. Copyright 2023, MDPI.

achieving relatively good results. Taking ISCO as an example, Zhong *et al.* reviewed the transition of persulfates from laboratory research to practical application [52]. As illustrated in Fig. 2, the mechanism of persulfate application during the ISCO process is shown. The method involves injecting activators and PMS into targeted groundwater or soil areas through injection wells, allowing reactions to occur within a controlled range. This method is an efficient strategy for controlling and remediating groundwater and soil contamination. Building on this, the section summarizes and compiles the most representative PMS treatment results for various types of characteristic groundwater and soil contaminants over the last five years, providing environmental restoration professionals with a clear and up-to-date reference guide categorized by pollutant type.

3.1. Heavy metal ions (HMIs)

AOPs have been significantly utilized in the remediation of heavy metal contamination in groundwater and soil. In soil, heavy metals can be classified into four fractions based on their speciation using the BCR method: The acid-soluble fraction (F1), the reducible fraction (F2), the oxidizable fraction (F3), and the residual fraction (F4) [53]. The interaction of PMS oxidative properties with heavy metal ions (HMIs) in the soil environment is a crucial area of study to enable precise removal of HMIs using PMS. Yang *et al.* conducted research on this topic and discovered that PMS treatment can convert heavy metals in soil (such as Cd^{2+}, Pb^{2+}, and Zn^{2+}) from a stable and difficult-to-degrade state to an active state, facilitating their subsequent removal through further treatment processes [54]. In soil, the inorganic forms of heavy metals are relatively stable. Yang *et al.* revealed that Pb^{2+} could react with SO_4^{2-} produced by PMS to form $PbSO_4$, and dislodge from the selected soil inorganic surrogate-montmorillonite clay. This demonstrates that PMS can address the challenging issue of inorganic heavy metal complexes that are difficult to degrade. Beyond the troublesome inorganic state, heavy metals also exist in soil bound in organic complexes. As expected, increasing concentrations of PMS led to more heavy metal ions being converted to their free states. Transforming the persistent heavy metals in soil into a more mobile form is crucial for facilitating subsequent remediation processes.

In actual contaminated systems, HMIs often form stable complexes with carboxylate ligands, which makes traditional remediation methods like chemical precipitation and adsorption less effective [55–57]. Compounding the problem, the reliance on reactive species such as $^{\bullet}OH$ and $^{\bullet}SO_4^-$ in AOPs for treating HMIs also becomes challenging. This is due to the low intrinsic degradation efficiency and the significant consumption of reactive species by coexisting substances (such as organics and carbonates) in wastewater. These factors have prompted researchers to shift their focus from direct degradation to exploring new alternative methods. Referencing the specific ligand-to-metal charge transfer (LMCT) for efficient removal of HMIs [58–61]. Yu *et al.* effectively degraded various Cu(II) complexes under the UV/PMS system [62]. The research found that the activation of UV/PMS produced a substantial amount of $^{\bullet}OH$ and $^{\bullet}SO_4^-$. These reactive species initially triggered the decarboxylation of Cu(II)-EDTA to form a Cu(II) intermediate, which further reacted with PMS to form a Cu(II) complex. Driven by LMCT, this led to the formation of Cu(I). Ultimately, Cu(III) was generated through a two-electron transfer process. The strong oxidizing nature of Cu(III) allowed it to rapidly attack the N–C bonds of Cu(II)-EDTA and its decarboxylation intermediates, thereby achieving the degradation of Cu(II), as illustrated in Fig. 3a. Simulation experiments on the degradation of Cu(II)-EDTA and Ni(II)-EDTA showed that the removal rates for Cu and Ni reached 100 % and 70 %, respectively, with actual chemical wastewater also achieving removal rates of approximately 100 % for Cu and over 50 % for Ni. In fact, the UV/PMS system also demonstrated high efficiency in treating other carboxylate ligands such as sodium citrate, tartrate, and NTA. This experiment on the *in-situ* generation and self-catalytic decomposition of endogenous Cu(III) and the strategy of using waste to treat waste merit further in-depth exploration. Xu *et al.* conducted degradation experiments on Cu-EDTA using four different metal ion catalyzed oxidation processes (MICOPs) and found that the Co^{II}/PMS system achieved degradation capabilities exceeding ppb levels under both acidic and alkaline conditions [63]. The oxidation decomposition pathway of EDTA is shown in Fig. 3b, and the results indicate that the chelate-breaking pathway of Co^{II}/PMS primarily follows Pathway 1. The experiments focused on the substitution mechanism of metal ions and concluded that it is highly correlated with the oxidation efficiency of MICOPs.

In literature review, we have observed that in the past five years, publications related to the PMS system and HMIs pollution have increasingly focused on complex pollution scenarios, specifically the coexistence of HMIs with organic pollutants. It appears that PMS does not act directly on HMIs during the treatment process. The primary mechanisms for the removal of HMIs are surface complexation and chemical precipitation, while the reactive species generated by PMS activation are more active against organic pollutants, such as norfloxacin (NOR) and polycyclic aromatic hydrocarbons (PAHs) [64,65]. The degradation processes for these different pollutants mutually enhance each other, creating a highly efficient synergistic effect. This type of reaction provides new insights into the removal of organics like antibiotics under environments containing heavy metal ions, further confirming the high efficiency of the PMS system in removing organic pollutants. These findings will be elaborated upon in detail later in the document.

3.2. Total petroleum hydrocarbon (TPHs)

As one of the characteristic pollutants in groundwater and soil, TPHs are often leaked into water bodies and soils due to the extraction processes of shale gas or the damage of diesel transmission equipment such as pipelines and storage tanks [66,67]. The impact on human ecosystems is severe and persistent, making the study of remediation for such pollution urgent. The zero-valent iron (ZVI, Fe^0) activated PMS system is a promising new development in the field of water and soil pollution treatment. As exemplified in Section 2.1, the O–O bond in PMS is broken, generating a substantial amount of $^{\bullet}OH$ and $^{\bullet}SO_4^-$ that participate in the degradation process. The choice of Fe^0 is strategic because, compared

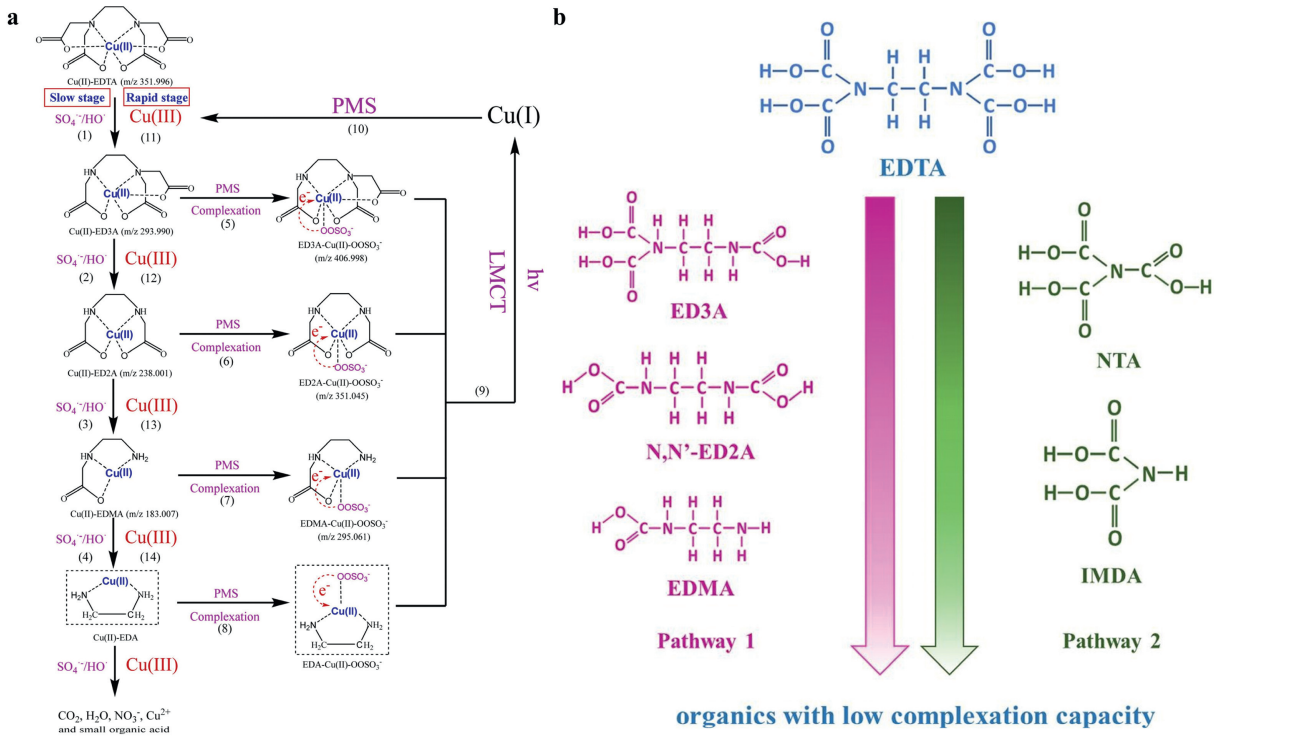


Fig. 3. (a) Cu(III) *in-situ* generation pathways, intermediates and their enhanced degradation by Cu(II)-EDTA, Reprinted with permission [62]. Copyright 2024, Elsevier. (b) General decomplexation pathways of EDTA and its complexes. Reprinted with permission [63]. Copyright 2020, Elsevier.

to Fe^{2+}, zero-valent iron has a longer lifespan and does not lead to the rapid quenching of ROS, enabling the sustained and high-energy production of ROS.

Jeong *et al.* used the PMS/nZVI system to treat diesel-contaminated soil, assessing its performance in degrading TPHs in the soil [68]. The optimal ratio was found to be 0.3 % PMS to 0.2 % nZVI, which reduced the TPH concentration from an initial 6625 mg/kg to 2573 mg/kg. $^{\bullet}OH$ and $^{\bullet}SO_4^-$ were identified as the primary ROS during the degradation process (thermal activation). After five successive applications of the 0.3 % PMS/0.2 % nZVI treatment, 96 % of TPH in the soil was successfully eliminated. This system demonstrates a broad pH applicability, and comparative experiments indicated that the effectiveness of different catalysts in activating PMS, and thus their performance in treating TPH, ranked as follows: nZVI > Fe(0) > Co(II) > Fe(II) > pure PMS. Furthermore, combinations of nZVI with different oxidizers were also tested in this contaminated system, with removal efficiencies ranking as follows: PMS > H_2O_2 > $KMnO_4$ > $Na_2S_2O_8$. Additionally, the activation mechanism of Fe^0 in this system was detailed by Mu's team, who divided it mainly into two types: Homogeneous activation of Fe^0 under acidic conditions, and heterogeneous activation on the surface of iron particles by the passivated Fe_2O_3. Both activation mechanisms ultimately produce the same ROS, namely $^{\bullet}OH$ and $^{\bullet}SO_4^-$. Mu's experiments discussed three advanced oxidation systems, finding that the oil removal performance of PMS/Fe^0 under acidic conditions was superior to that of H_2O_2/Fe^0 and PDS/Fe^0.

Beyond the exceptional activation performance of ZVI, FeS and pyrite (FeS_2) have gradually come into the focus of researchers in recent years. The electron-donating characteristics of sulfur can significantly enhance the reactivity of catalysts. More importantly, S(II) serves as a source of energy for the transition of iron valence states [69,70], and it is one of the main reasons for the continuous production of $^{\bullet}SO_4^-$, the primary oxidizing agents during the degradation process. A graphene-based catalyst (GBC), created from a combination of FeS, Cu^0, and waste soybean residue biomass precursors with PMS, removed over 90 % of TPHs within

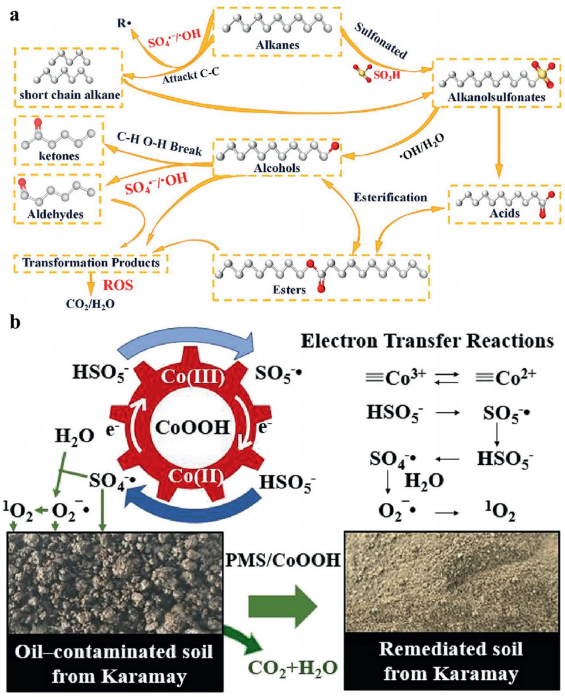


Fig. 4. (a) Proposed degradation pathway of alkanes in petroleum hydrocarbons. Reprinted with permission [71]. Copyright 2023, Elsevier. (b) Possible mechanism of soil remediation by PMS/CoOOH and schematic comparison of soil before and after remediation. Reprinted with permission [73]. Copyright 2019, Elsevier.

180 min (thermal activation) [71]. The proposed degradation pathway of alkanes in petroleum hydrocarbons can be referenced as in Fig. 4a. Pyrite, coupled with PMS and heterotrophic ammonium assimilation (HAA) in a pre-oxidation treatment system, achieved removal rates of 96.9 % for TPHs and 98.3 % for ammonia (NH_4^+-N)

[72]. The various ROS produced during the degradation process, including $^{\bullet}SO_4^-$, $^{\bullet}OH$, $^{\bullet}O_2^-$, and $^1O_2$, facilitated the oxidative degradation of long-chain alkanes, alcohols, and esters through radical and non-radical pathways.

Like the PMS/Fe system, the PMS/Co system is promising, but given the toxicity of cobalt ions, it is crucial to find cobalt-based catalysts that are environmentally friendly, structurally stable, and exhibit excellent catalytic performance. Surprisingly, cobalt-containing materials have been very active in the field of PMS activation for the degradation of petroleum hydrocarbons in recent years. Wang *et al.* utilized cobalt hydroxide (CoOOH) to activate PMS through chemical oxidation, aiming to remediate petroleum-contaminated soil [73]. With an input of 1.0 g/L CoOOH and 0.1 mol/L PMS, 88.3 % of the initial grease concentration (thermal activation), ranging from 78 mg/kg to 99 mg/kg, was removed within 24 h. The removal rate of total organic carbon (TOC) reached 73 %, with sulfate radicals, hydroxyl radicals, and singlet oxygen participating in the oxidation reaction. Moreover, the CoOOH used in the reaction could be recycled, preventing secondary pollution. The reaction process and the before-and-after effects on the soil are depicted in Fig. 4b. In the realm of precise control, due to the inability of single atoms to simultaneously satisfy the adsorption of PMS and pollutants and the formation of ROS, Yang *et al.* developed a dual-atomic dispersed active site anchoring method [74]. This method involved synthesizing a visible-light-responsive Co-Mn/CN catalyst, defining the coordination environment of $CoN_4{-}MnN_2$, and elucidating the catalytic mechanism for the all-day activation and degradation of petroleum hydrocarbons by PMS at the atomic scale. The differing electronic structures and coordination environments of the dual atoms led to adjustments in the d-band center, thereby optimizing the adsorption process of intermediates. The Co-Mn/CN DACs system effectively converted PMS into $^1O_2$, while $^{\bullet}SO_4^-$ and $^{\bullet}OH$ still played key roles in the reaction. DFT calculations indicated the transformation pathway as: $^* + PMS \rightarrow {}^*OH{}^*SO_4 \rightarrow {}^*OH \rightarrow 2{}^*OH \rightarrow {}^*O \rightarrow 2{}^*O \rightarrow {}^*O\text{-}O^* \rightarrow {}^1O_2$. The synergistic effect enhanced the catalytic activity of Co and Mn, achieving a PMS utilization rate of 86.5 %. The optimal PMS dosing was 0.4 mol/L, with the most suitable pH condition being 7, which also showed broad pH adaptability. The degradation rates for C14 reached 80.0 % and 82.2 %, respectively.

3.3. Benzene derivatives (BTEX)

Benzene derivatives, which are highly mobile and volatile, are classified as volatile organic compounds (VOCs) and are significant characteristic pollutants in chemical industrial parks [75]. Typical contaminants include benzene, toluene, and xylene. Recent studies have shown that PMS, commonly used as a radical precursor in AOPs, outperforms H_2O_2 in the removal of BTEX [76,77]. This is because sulfate radicals possess a higher oxidation–reduction potential ($E_0 = 2.5$–3.1 eV), offering greater selectivity and enhanced capabilities for decomposition and mineralization of VOCs. A search of recently published results revealed that Co and Fe are more active among the transition metals that can be used to activate the PMS/AOPs process for BTEX contamination. Whether it is the synthesis of Mn-Co bimetallic spinel catalysts and activation of PMS, which stably removed 97.3 % of toluene within 25 h [78]. In this process, $^{\bullet}O_2^-$, $^1O_2$, $^{\bullet}OH$ and $^{\bullet}SO_4^-$ were identified the primary free radicals generated in this reaction system. $^{\bullet}O_2^-$ was superior to other radicals in both initial decomposition and mineralization of toluene; $^{\bullet}SO_4^-$ was mainly to accelerate the ring-opening of toluene; while $^1O_2$ and $^{\bullet}OH$ mainly contributed to the further degradation of small organic compounds (Fig. 5a). The doping of CN by Co atoms to form CCN catalysts with Co-N configuration together with PMS with toluene removal rate of >90 % for 7 consecutive days [79], which can generate plenty $^1O_2$, it was because the

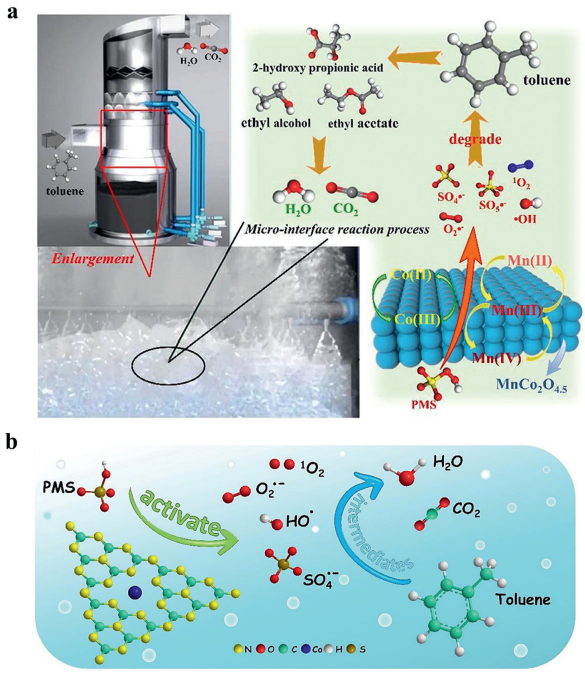


Fig. 5. (a) Schematic of toluene degradation by using $MnCo_2O_{4.5}$/PMS system. Reprinted with permission [78]. Copyright 2023, Elsevier. (b) The possible generation mechanism of ROS for toluene degradation in Co-CN/PMS system. Reprinted with permission [79]. Copyright 2024, Elsevier.

electron transferred from Co atom to PMS in the activation process (Fig. 5b). In addition, the co-catalysis of mixed VOCs (chlorobenzene, styrene, toluene) by MoS_2 and Fe^{3+}/PMS or the efficient treatment of mixed VOCs (chlorobenzene, styrene, toluene) by co-catalysis of MoS_2 and Fe^{3+}/PMS [80], or the generation of CX_3R-type oxidative by-products (OBPs) by $^{\bullet}SO_4^-$ in the AOPs reaction, and their degradation by the addition of the Co^{2+}/PMS system to achieve complete environmental remediation [81]. In summary, all of the above are the excellent performance of Co and Fe demonstrated in the field of BTEX remediation.

Beyond the activation of PMS by transition metals, Kirill *et al.* proposed a novel approach using hydrodynamic cavitation (HC) technology to activate PMS (Schematic diagram of device is shown in Fig. 6a) [82]. In the experiments, the degradation capabilities of HC-PMS and HC-PS systems were compared for benzene, toluene, ethylbenzene, and *o*-xylene. The degradation results showed that within 240 min, the degradation rates for BTEX in the two systems were 90.85 %, 94.50 %, 94.36 %, 93.07 % for HC-PMS, and 91.51 %, 95.50 %, 94.65 %, 94.95 % for HC-PS respectively. Although the degradation rates of PMS were slightly lower than those of PS, the degradation kinetics of PMS were faster than those of the PS system. BTEX was oxidatively degraded through four steps: H-abstraction, $^{\bullet}OH$ addition, dealkylation, and final mineralization. Furthermore, Kirill made an intriguing discovery that the presence of Cl^- significantly enhanced the degradation efficiency of BTEX. This finding suggests a synergistic interaction between $^{\bullet}SO_4^-$ and Cl^-, highlighting the potential of HC as an effective method for environmental remediation of VOCs. In addition to proposing HC technology, Kirill also pioneered the association of asphaltenes (Asph) with PMS activation [83], conducting simultaneous degradation of mixed BTEX (benzene, toluene, ethylbenzene, and *o*-xylene) under US irradiation. The removal rates achieved were 76 %, 91 %, 97 %, and 97 % respectively. Asph in the system function by generating additional cavitation event centers, which aid in the formation of ROS. Furthermore, asphaltenes interact with the benzene rings in BTEX through π-π stacking interac-

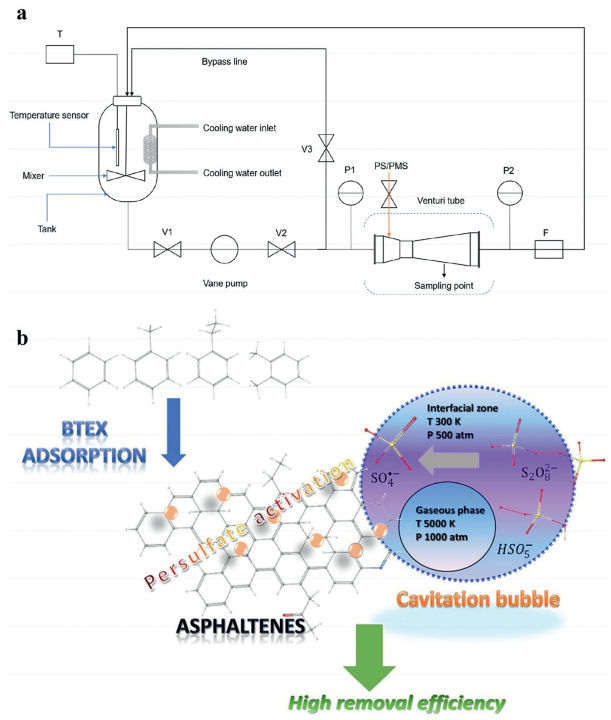


Fig. 6. (a) Schematic diagram of the device for HC technology. Reprinted with permission [82]. Copyright 2024, Elsevier. (b) ROS and path during degradation of BTEX by Asphaltenes. Reprinted with permission [83]. Copyright 2020, Elsevier.

tions. In the PMS/US/Asph system degrading BTEX, $^{\bullet}SO_4^-$ and $^{\bullet}OH$ play primary roles, while $^{\bullet}O_2^-$ serve a secondary role. The oxidative reaction is depicted in Fig. 6b, illustrating the dynamics and interactions at play in the degradation process.

3.4. Chloroalkane ((Ar)R-Cl)

Chloroalkane is diverse and complex; however, this review focuses only on typical chlorinated hydrocarbon pollutants found in the groundwater/soil of chemical industrial parks. Due to their persistence, mobility, and volatility, (Ar)R-C are of particular concern. Research over the past five years indicates that many groups working with PMS/AOPs systems have been investigating the synthesis or activation methods of catalysts for the degradation of trichloroethylene (TCE). Activation systems utilizing FeS or FeS_2 in conjunction with PMS exhibit outstanding efficacy. Direct application of FeS_2 to activate various oxidizing systems [84], specifically FeS_2/PMS, FeS_2/PS, and FeS_2/H_2O_2, results in degradation efficiencies for TCE of 99.84 %, 99.63 %, and 98.47 %, respectively. Due to the inherent pH buffering properties of FeS_2, these systems demonstrate robust resistance to pH variations, which enhances their operational stability. Detailed electron paramagnetic resonance (EPR) testing and analyses using sacrificial agents confirm that $^{\bullet}SO_4^-$ and $^{\bullet}OH$ play pivotal roles in facilitating these high degradation rates. Further investigations into the degradation capabilities for other chlorinated hydrocarbons indicate that FeS_2/PMS systems are particularly effective against TCE and perchloroethylene (PCE), with removal efficiencies of 99.63 % and 99.93 %, respectively. However, the effectiveness against 1,1,1-trichloroethane (TCA), 1,2,3-trichloropropane (TCP), and dichloroethane (DCA) is significantly lower, with removal rates not exceeding 32 %. In an extension of this research, Habib synthesized iron sulfide nanoparticles (FeS-NPs), which when used in conjunction with PMS, achieved a TCE removal rate of 82.63 % [85]. Building on this foundation, Sun explored a novel catalyst composed of reduced graphene oxide-supported nano zero-valent iron (nZVI) with FeS anchored on it (FeS@nZVI-rGO) [86]. This innovative catalyst configuration, primarily driven by the activity of $^{\bullet}SO_4^-$ and $^{\bullet}OH$, achieves >85 % removal of TCE. Notably, the anchoring of FeS onto the catalyst mitigates the corrosion of active sites and iron loss, thereby significantly enhancing the lifespan and sustainability of the system.

Recent advances in the development and study of heterogeneous catalysts for degradation processes have been notable. Deng *et al.* discussed the Ni-Fe (hydr)oxides system, which demonstrated an efficient degradation of TCE with 96.8 % removal within 40 min [87]. At the initial stage of the reaction, the nonradical pathway prevails. This pathway generates high-valent metals and $^{\bullet}SO_4^-$, and indirectly produces $^1O_2$. $^1O_2$ and dissolved O_2 together participate in the O_2 cycling, the generation of $^{\bullet}OH$, and the electron transfer process that involves the reduction of trivalent metals. In the later stage, divalent metals react with PMS *via* the radical pathway. This reaction leads to the generation of highly oxidative $^{\bullet}OH$ and $^{\bullet}SO_4^-$ (Fig. 7a). Liu *et al.* developed a cobalt iron oxide loaded on cerium dioxide (CeO_2) surface, specifically the $Co_{1.5}Fe_{1.5}O_4$-CeO_2/PMS system, which exhibited the capability to process over 90 % of pollutants such as TCE, carbon tetrachloride (CT), and dichloromethane (DCM) [88]. Co is the main active substance for PMS activation, and the valence cycle of Fe/Co/Ce accelerates the catalytic activity of PMS. $Co_{1.5}Fe_{1.5}O_4$-CeO_2/PMS system has better pH tolerance and environmental adaptability. Multiple rapid recovery experiments show that the catalyst has excellent recyclability and stable structure ensures its recovery rate. In addition, the introduction of CeO_2 changed the activation mechanism of $Co_{1.5}Fe_{1.5}O_4$/PMS, and the active substance that degrades TCE changed from free radical pathway to dual-track system, which is conducive to coping with complex water environment (Fig. 7b). Feng *et al.* made progress with cubic spinel catalysts (M_2MnO_4), achieving broad pH adaptability and low metal dissolution rates with MMn_2O_4 and M_2MnO_4 systems (M= Fe, Cu, Zn, Co) (Fig. 7c). The optimal sample demonstrated an efficiency of 99.9 % TCE removal within 5 min [89]. An increase in the charge density within the cubic spinel structure can effectively expedite the redox cycles between high and low metal valence states. This process ensures the efficient activation of PMS. As a result, free radicals such as $^{\bullet}OH$ and $^{\bullet}SO_4^-$ are fully generated. These free radicals play a crucial role in promoting the degradation of TCE, facilitating a more rapid and complete breakdown of this contaminant (Fig. 7d). Wang *et al.* synthesized manganese, cobalt, and oxygen co-doped graphitic carbon nitride (MCOCN) which was capable of removing TCE completely (100 %) within 10 min without pH adjustment (Fig. 7e) [90]. It is evident that $SO_4^{\bullet-}$ and $^{\bullet}OH$ play a primary role in most of these degradation processes, with $^{\bullet}O_2^-$ and $^1O_2$ also contributing in some cases. The reaction mechanisms mentioned above, as well as additional details including the valence state transitions of transition metals, degradation pathways, and schematic diagrams of special structures, can be found in Fig. 7e. This figure also encompasses some of the details not elaborated upon in the text, providing a comprehensive overview of the involved processes. Research on the activation of PMS has garnered widespread attention, yet Zhao *et al.* has considered the cost and energy consumption associated with the activation process [91]. As such, they explored the feasibility of using non-activated PMS for the advanced oxidation treatment of TCE in soil through degradation tests. The results indicated that a single injection of PMS could degrade 86.9 % of total TCE in the soil, while continuous injection increased the removal rate to 95.25 %. This study highlights the potential of non-activated PMS to degrade TCE in soil through a direct and continuous oxidation reaction, particularly demonstrating enhanced performance in the treatment of soil with high concentrations of TCE.

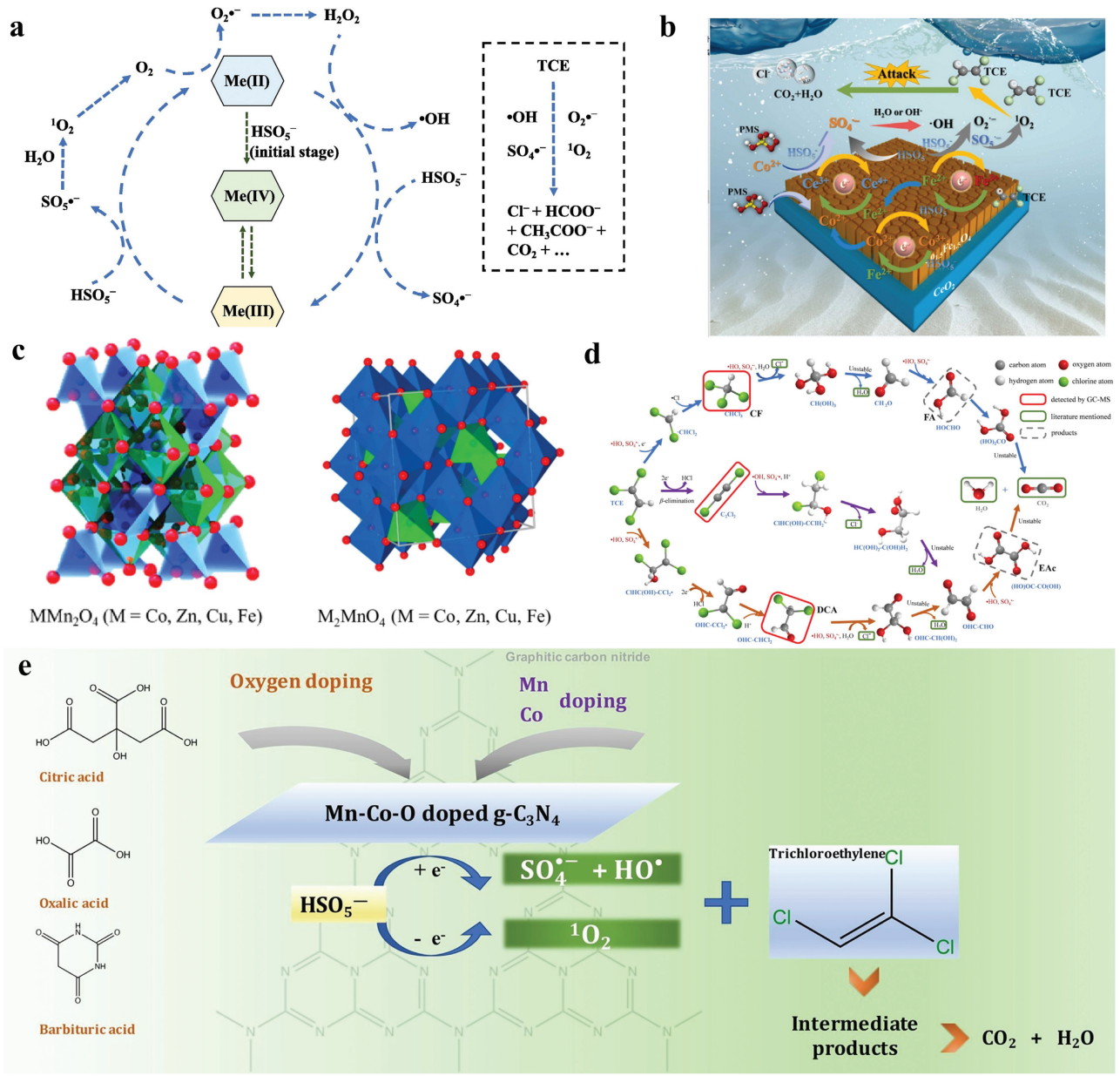


Fig. 7. (a) Degradation mechanism diagrams: Ni-Fe (hydro)oxide/PMS system. Reprinted with permission [87]. Copyright 2023, Elsevier. (b) $Co_{1.5}Fe_{1.5}O_4$–CeO_2/PMS system. Reprinted with permission [88]. Copyright 2024, Elsevier. (c) Structural diagrams of MMn_2O_4 tetragonal spinel and M_2MnO_4 cubic spinel. (d) Degradation pathway diagrams of the $M_xMn_{3-x}O_4$ (M = Co, Zn, Cu, Fe; x = 1, 2)/PMS system for TCE. (c, d) Reprinted with permission [89]. Copyright 2022, Elsevier. (e) Synthesis and degradation mechanism of MCOCN. Reprinted with permission [90]. Copyright 2021, Elsevier.

4. Conclusion, challenges and outlook

Peroxymonosulfate (PMS) has garnered significant attention as a potential oxidant and is increasingly being used in AOPs for remediating contaminated groundwater and soil in chemical industrial parks. This mini-review specifically addresses the activation methods of PMS, detailing four representative techniques: transition metals, heat, irradiation, and alkalinity. It provides an overview of the mechanisms involved and the pathways for ROS generation. Given the feasibility of implementation at actual sites, alkaline and iron-based activation technologies are the most commonly applied in field applications. In recent years, coupled activation has emerged as a trend in the development of AOPs. Combining the advantages of various activation methods to offset the disadvantages of individual technologies remains an area that requires further exploration. Although, this approach could enhance the efficiency and adaptability of PMS activation for environmental remediation tasks.

There are still many difficult challenges in the application of PMS-based AOPs to the treatment of groundwater pollutants in chemical parks, as follows:

(1) The composition of groundwater pollutants in the chemical industry park is complex, including various organic pollutants and heavy metals. The reactivity of different pollutants varies greatly, and some organic compounds with complex structures are extremely difficult to be oxidized and degraded. The concentration span of pollutants is large, high concentration requires a large number of oxidants and a long reaction time, and low concentration is difficult to effectively trigger the reaction. And there are many persistent organic pollutants such as polychlorinated biphenyls that resist degradation.

(2) At the technical application level, the selectivity of free radical reaction is poor, often reacts needlessly with other substances in groundwater, reduces the treatment efficiency, and may produce harmful by-products.
(3) The mass transfer process is limited, which affects the full contact between pollutants and oxidants and catalysts. Light-dependent technologies also suffer from poor light penetration.
(4) Environmental factors can not be underestimated, complex geological conditions affect the diffusion of oxidants, groundwater pH, hardness and other water quality conditions interfere with the reaction, microorganisms will also interact with the oxidation process.
(5) The processing cost is high, the equipment investment, oxidizer and power consumption are huge, and the professional operation and maintenance requirements are high, the need for professionals to real-time monitoring and accurate regulation of reaction conditions, this series of problems need to be solved.

Declaration of competing interest

The authors declare that they have no known competing financial interests or personal relationships that could have appeared to influence the work reported in this paper.

CRediT authorship contribution statement

Yingnan Duan: Writing – original draft. **Jinyu Liu:** Writing – original draft. **Qian Liu:** Writing – review & editing. **Tianhao Li:** Writing – review & editing. **Hexiang Zhao:** Writing – review & editing, Writing – original draft. **Zhurui Shen:** Writing – review & editing, Writing – original draft.

Acknowledgments

This work was supported by the National Key Research and Development Program of China (No. 2023YFC3708005), the National Natural Science Foundation of China (Nos. 21872102, 22172080) and the Fundamental Research Funds for the Central Universities (Nankai University, No. 63241208).

References

[1] J.B. Zhang, C. Dai, Z. Wang, et al., Water Res. 244 (2023) 120555.
[2] X. Kuang, J. Liu, B.R. Scanlon, et al., Science 383 (2024) eadf0630.
[3] C. Liu, S. Liu, L. Liu, et al., Chem. Eng. J. 379 (2020) 122274.
[4] J. Li, Y. Li, Z. Xiong, et al., Chin. Chem. Lett. 30 (2019) 2139–2146.
[5] Y. Liu, F. Shan, H. Yue, et al., J. Environ. Manage. 333 (2023) 117460.
[6] X. Shu, L. Xu, M. Yang, et al., Sci. Total Environ. 868 (2023) 161578.
[7] N. Li, Y. Wang, X. Cheng, et al., Water Res. 222 (2022) 118896.
[8] A. Edet, E. Nyong, A. Ukpong, et al., Sustain. Wat. Resour. Manag. 7 (2021) 50.
[9] S. Zhu, Y. Wu, Z. Qu, et al., J. Clean Prod. 247 (2020) 119140.
[10] H. Zhao, Y. Wang, J. Yang, et al., Chem. Eng. J. 454 (2023) 140297.
[11] A. Tewari, P.P. Paroha, S. Awasthi, Orient. J. Chem. 38 (2022) 1428–1434.
[12] C. Lu, Y. Chen, C. Shuang, et al., Water Res. 250 (2024) 121000.
[13] G. Galvagno, C. Eskicioglu, M. Abel-Denee, Water Res. 96 (2016) 84–93.
[14] L. Shi, Z. Hu, Y. Wang, et al., Chem. Eng. J. 413 (2021) 127485.
[15] Y. Chen, S. Lan, M. Zhu, Chin. Chem. Lett. 32 (2021) 2052–2056.
[16] M. Mahdi-Ahmed, S. Chiron, J. Hazard. Mater. 265 (2014) 41–46.
[17] T. Zhang, C. Zhang, H. Zhang, ChemCatChem 17 (2024) e202401359.
[18] Q. Fang, H. Yang, S. Ye, et al., Water Res. 245 (2023) 120614.
[19] C. Guo, M. Cheng, G. Zhang, et al., Environ. Sci.: Nano 10 (2023) 1528–1552.
[20] H. Luo, H. Fu, H. Yin, et al., J. Hazard. Mater. 426 (2022) 128044.
[21] T. Liu, B. Yao, Z. Luo, et al., Sci. Total Environ. 836 (2022) 155421.
[22] R. Wen, G. Shen, L. Meng, RSC Adv. 13 (2023) 24565–24575.
[23] H. Zheng, Y. Hou, S. Li, et al., Chin. Chem. Lett. 33 (2022) 5013–5022.
[24] E.M. Abd El-Monaem, H.M. Elshishini, S.S. Bakr, et al., npj Clean Water 6 (2023) 34.
[25] D.T. Oyekunle, E.A. Gendy, J. Ifthikar, et al., Chem. Eng. J. 437 (2022) 135277.
[26] J. Ma, N. Ding, H. Liu, Sep. Purif. Technol. 324 (2023) 124628.
[27] K. Zhi, Z. Li, P. Ma, et al., Appl. Sci. 11 (2021) 11314.
[28] B. Li, Y.F. Wang, L. Zhang, et al., Chemosphere 291 (2022) 132954.
[29] B. Liu, B. Huang, Z. Wang, et al., J. Environ. Chem. Eng. 11 (2023) 109586.
[30] X. Zheng, X. Niu, D. Zhang, et al., Chem. Eng. J. 429 (2022) 132323.
[31] B. Shao, Y. Xu, Z. Liu, et al., J. Clean Prod. 384 (2023) 135518.
[32] Z. Honarmandrad, X. Sun, Z. Wang, et al., Water Resour. Ind. 29 (2023) 100194.
[33] J. You, J. Li, H. Zhang, et al., J. Hazard. Mater. 445 (2023) 130440.
[34] L. Hao, C. Guo, Z. Hu, et al., Nanoscale 14 (2022) 13861–13889.
[35] H. Liu, Z. He, S. Wang, et al., Chem. Eng. J. 469 (2023) 144054.
[36] Y. Mao, Y. Wu, X. Lu, et al., Chem. Eng. J. 453 (2023) 139723.
[37] S. Zou, Q. Chen, Y. Liu, et al., Chin. Chem. Lett. 32 (2021) 2066–2072.
[38] Z. Wang, W. Qiu, S. Pang, et al., Water Res. 172 (2020) 115504.
[39] K. Ulucan-Altuntas, S. Yazici Guvenc, E. Can-Güven, et al., Environ. Sci. Pollut. Res. 29 (2021) 9110–9123.
[40] J. Wang, S. Wang, Chem. Eng. J. 334 (2018) 1502–1517.
[41] D. Zhao, X. Liao, X. Yan, et al., J. Hazard. Mater. 254-255 (2013) 228–235.
[42] T. Song, G. Li, R. Hu, et al., Catalysts 12 (2022) 1025.
[43] L. Shen, H. Wang, J. Kang, et al., Chem. Eng. J. 474 (2023) 145837.
[44] S. Wang, J. Wang, Chem. Eng. J. 336 (2018) 595–601.
[45] H. Wang, B. Liu, Q. Si, et al., Environ. Funct. Mater. 1 (2022) 21–33.
[46] C. Qi, X. Liu, J. Ma, et al., Chemosphere 151 (2016) 280–288.
[47] S.K. Gujar, G. Divyapriya, P.R. Gogate, et al., Crit. Rev. Environ. Sci. Technol. 53 (2022) 780–802.
[48] J. Du, C. Wang, M. Sun, et al., J. Hazard. Mater. 463 (2024) 132916.
[49] T. Zeng, X. Tang, X. Cai, et al., ACS Catal. 14 (2024) 1405–1418.
[50] J. Yang, M. Zhang, M. Chen, et al., Adv. Mater. 35 (2023) 2209885.
[51] J. Yan, L. Gong, S. Chai, et al., Chem. Eng. J. 458 (2023) 141456.
[52] Y. Li, G. Liu, J. He, et al., Appl. Sci. 13 (2023) 1304.
[53] L. Liu, L. Huang, R. Huang, et al., J. Hazard. Mater. 403 (2021) 123648.
[54] L. Zhang, L. Long, Q. Zhu, et al., Sci. Total Environ. 926 (2024) 171717.
[55] Z. Zhou, C. Zhang, M. Xi, et al., Water Res. 238 (2023) 120007.
[56] D. Zu, H. Song, C. Li, et al., Appl. Catal. B: Environ. 306 (2022) 121131.
[57] Y. Yuan, W. Zhao, Z. Liu, et al., Water Res. 171 (2020) 115375.
[58] S. Sun, S. Wang, Y. Ye, et al., Water Res. 153 (2019) 21–28.
[59] Z. Xu, G. Gao, B. Pan, et al., Water Res. 87 (2015) 378–384.
[60] S. Wang, B. Zhang, Y. Fei, et al., Environ. Sci. Technol. 57 (2023) 19921–19931.
[61] J. He, B. Zhang, C. Tan, et al., Water Res. 265 (2024) 122248.
[62] J. Yu, W. Deng, X. Huang, et al., J. Hazard. Mater. 465 (2024) 133521.
[63] Z. Xu, T. Wu, Y. Cao, et al., Chem. Eng. J. 392 (2020) 123639.
[64] X. Zhang, X. Zhang, C. An, et al., Sep. Purif. Technol. 311 (2023) 123341.
[65] Z. Chu, H. Liu, T. Chen, et al., J. Environ. Chem. Eng. 12 (2024) 112048.
[66] J.T. McGuire, I.M. Cozzarelli, B.A. Bekins, et al., Environ. Sci. Technol. 52 (2018) 12172–12178.
[67] Y. Li, B. Zheng, Y. Yang, et al., J. Hazard. Mater. 436 (2022) 129231.
[68] R. Bajagain, S.W. Jeong, Chemosphere 270 (2021) 128627.
[69] J. Qu, Y. Xu, X. Zhang, et al., Appl. Catal. B: Environ. 316 (2022) 121639.
[70] Q. Hong, C. Liu, Z. Wang, et al., Chem. Eng. J. 417 (2021) 129238.
[71] J. Lei, Y. Han, C. Zhao, et al., Sep. Purif. Technol. 324 (2023) 124591.
[72] C. Zhao, J. Lei, F. Han, et al., Water Res. 247 (2023) 120772.
[73] C. Lyu, D. He, Y. Chang, et al., Sci. Total Environ. 680 (2019) 61–69.
[74] Q. Guo, X. Yu, K. Zhang, et al., Appl. Catal. B: Environ. 343 (2024) 123581.
[75] F. Bi, Z. Zhao, Y. Yang, et al., Environ. Funct. Mater. 1 (2022) 166–181.
[76] R. Xiao, L. He, Z. Luo, et al., Sci. Total Environ. 710 (2020) 136333.
[77] L. Gao, Q. Mao, S. Luo, et al., Environ. Pollut. 259 (2020) 113795.
[78] S. Wang, S. Liu, X. Chen, et al., Chem. Eng. J. 453 (2023) 139901.
[79] H. Miao, X. Zhang, X. Zhang, et al., Chem. Eng. J. 485 (2024) 149743.
[80] X. Xie, Y. Xiang, J. Cao, et al., Sep. Purif. Technol. 305 (2023) 122444.
[81] T. Chen, Z. Yu, T. Xu, et al., J. Hazard. Mater. 405 (2021) 124243.
[82] K. Fedorov, X. Sun, G. Boczkaj, Chem. Eng. J. 417 (2021) 128081.
[83] K. Fedorov, M. Plata-Gryl, J.A. Khan, et al., J. Hazard. Mater. 397 (2020) 122804.
[84] M. Habib, M. Ali, T. Ayaz, et al., Environ. Pollut. 333 (2023) 122062.
[85] M. Habib, T. Ayaz, M. Ali, et al., J. Water Process. Eng. 58 (2024) 104922.
[86] Y. Sun, M. Gu, S. Lyu, et al., J. Hazard. Mater. 392 (2020) 122328.
[87] J. Deng, W. Chen, F. Wu, et al., Sep. Purif. Technol. 325 (2023) 124675.
[88] B. Liu, J. Li, C. Wang, et al., J. Environ. Chem. Eng. 12 (2024) 112280.
[89] M. Feng, Z. Xu, X. Bai, et al., Chem. Eng. J. 446 (2022) 137394.
[90] Y. Wang, L. Fang, Z. Wang, et al., Sep. Purif. Technol. 278 (2021) 119580.
[91] B.T. Oba, X. Zheng, M.A. Aborisade, et al., J. Environ. Manage. 285 (2021) 112063.